CONCEPT AND CHARACTERISTICS OF A SIMULATED LINE SOURCE FOR ANNULAR BLANKET EXPERIMENTS USING AN ACCELERATOR-BASED DEUTERIUM-TRITIUM NEUTRON SOURCE

BLANKET ENGINEERING

KEYWORDS: *line source simulation, annular blanket, tokamak fusion reactor*

Y. OYAMA, C. KONNO, Y. IKEDA, K. KOSAKO, H. MAEKAWA, and T. NAKAMURA *Japan Atomic Energy Research Institute*
Department of Reactor Engineering, Tokai Research Establishment
Tokai-mura, Naka-gun, Ibaraki-ken, 319-11 Japan

M. A. ABDOU *University of California, Los Angeles,*
School of Engineering and Applied Science
Mechanical, Aerospace, and Nuclear Engineering Department
Los Angeles, California 90095

E. F. BENNETT *Argonne National Laboratory, Fusion Power Program*
Building 205, 9700 South Cass Avenue, Argonne, Illinois 60439

A. KUMAR, Y. WATANABE,* and M. Z. YOUSSEF
University of California, Los Angeles
School of Engineering and Applied Science
Mechanical, Aerospace, and Nuclear Engineering Department
Los Angeles, California 90095

Received January 28, 1994
Accepted for Publication July 28, 1994

A pseudoline source is realized by using an accelerator-based deuterium-tritium point-neutron source. The pseudoline source is obtained by time averaging of the continuously moving point source or by superposition of the finely distributed point sources. The line source is utilized for fusion blanket neutronics experiments with an annular geometry to simulate a part of a tokamak reactor. The source neutron characteristics are measured for two operational modes for the line source: the continuous and the stepwise modes, with activation foil and NE-213 detectors, respectively. The neutron source characteristic is calculated by a Monte Carlo code to give a source condition for a successive calculational analysis of the annular blanket experiment. The reliability of the Monte Carlo calculation is confirmed by comparison with the measured source characteristics.

*Current address: University of Florida, Department of Nuclear Engineering Sciences, Room 202, Nuclear Science Center, Gainesville, Florida 32611.

I. INTRODUCTION

The idea of a cylindrical geometry that uses a line source and an annular test assembly can be easily reached by consideration of neutronic tests with fusion reactor geometry. A spherical geometry with a point neutron source is analogous to inertial fusion systems such as laser fusion while a cylindrical geometry with a line neutron source leads us to simulation of magnetic fusion systems such as mirror and tokamak machines.

Conceptual designs of a cylindrical assembly with a line source appeared in early studies for the AYMAN project by Sahin and Kumar,[1] Sahin and Al-Kusayer,[2] and Sahin et al.[3] and for the Fusion Reactor Blanket Facility (FRBF) by Beller et al.[4] Sahin proposed an experimental arrangement that was mainly for a fusion-fission hybrid configuration in cylindrical geometry and compared various radial compositions for nuclear performances such as fissile and fusile fuel production with a close examination of experimental prospects. He assumed a movable point source for simulating the line source, but he did not give a technical explanation for realization of the means and the experimental prospect of relating source characteristics. Using a line source with a cosine-shaped intensity profile, Beller reported a conceptual design of a cylindrical blanket system. The source design consisted of a deuteron beam, introduced through a slit on the side of the target, sweeping over an elongated target. Using blanket compositions from the design study of the Blanket Comparison and Selection Study,[5] Beller discussed the neutronic evaluation of two azimuthal effects of neutron energy and yield variations by a line source introduced from the side slit in the blanket. He pointed out, though it seems optimistic, that the advantages of is proposal were flexibility for experimental configurations and separability of the flux in the radial and the axial directions.

Neutronics tests for annular blankets with a line source were planned for the third part (Phase-III) of the Japan Atomic Energy Research Institute (JAERI)/U.S. Department of Energy (U.S. DOE) collaborative program on fusion blanket neutronics.[6] These experiments aimed at obtaining three-dimensional benchmark data for fusion reactor design codes and nuclear data libraries. Because the experiments were desired for better simulation of the fusion reactor environment relevant to toroidal geometry, a volumetric source was introduced instead of a point neutron source. Thus, there was motivation for the development of a line deuterium-tritium (D-T) neutron source. The most difficult problem was to produce a line source uniformly with minimum distortion. Because the primary azimuthal neutron energy spectrum and yield distributions depend on the emission angle as far as the point neutron source, a deuteron accelerator and a tritium metal target system were applied. To construct the line source, one needed to take into account not only technical feasibility but also development cost. From these considerations, a pseudoline source system was constructed at the Fusion Neutronics Source (FNS) facility[7] at JAERI. This paper describes the method for generating the line source and the associated equipment and discusses the characteristics of the line source.

II. LINE SOURCE PREPARATION

II.A. Realization of Line Source

The accelerator-based D-T point neutron source FNS was utilized to realize a pseudoline source. A continuous forth-and-back motion of the test blanket relative to a fixed point source can give a line source by time averaging when an observation is made of the detectors moving together with the test blanket. This is the pseudoline source because it is effective only by time averaging, although this superposition could not be applied for a time-dependent response such as activation with a short decay time. Obtaining a uniform distribution of source intensity requires a constant moving speed and a constant neutron generation rate during the shuttle motion of the test blanket. However, a beam current of accelerated deuterons is not perfectly controlled for adjustment of the moving speed of the test blanket to keep a uniform neutron yield distribution. Hence, a stepwise operation mode, in addition to the continuous operation mode, was derived by superposition of the collected data with postprocessing from a finite number of neutron source points. In the case of a stepwise mode, because the measurement is performed during the staying of the source, the neutron yield can be normalized at each position. The continuous mode can be operated by using a servomotor to drive the deck with constant speed while the stepwise mode needs to accurately stop the test blanket at the desired positions.

A calculational study of the stepwise operation mode showed that there are a minimum number of points that are enough to represent the equivalent line source.[8] When a 2-m-long line source was considered, the analysis indicated that the speed of the moving point source should be faster than 1.2 mm/s in the case of induced activity measurement with a half-life shorter than 10 h. This is discussed later, but most of the activation measurements practically used have such a half-life range. In the case of the stepwise operation, when the source interval was <125 mm, the analysis also showed that the deviation of the neutron flux around this line source from that of an ideal line source was $<0.1\%$. With these considerations, the specifications of equipment for a line source were determined, and a control system and measurement scheme were designed.

II.B. Design and Operation Control of Carriage Deck System

The basic idea of the line source device that was designed is shown in Fig. 1. The device included a long

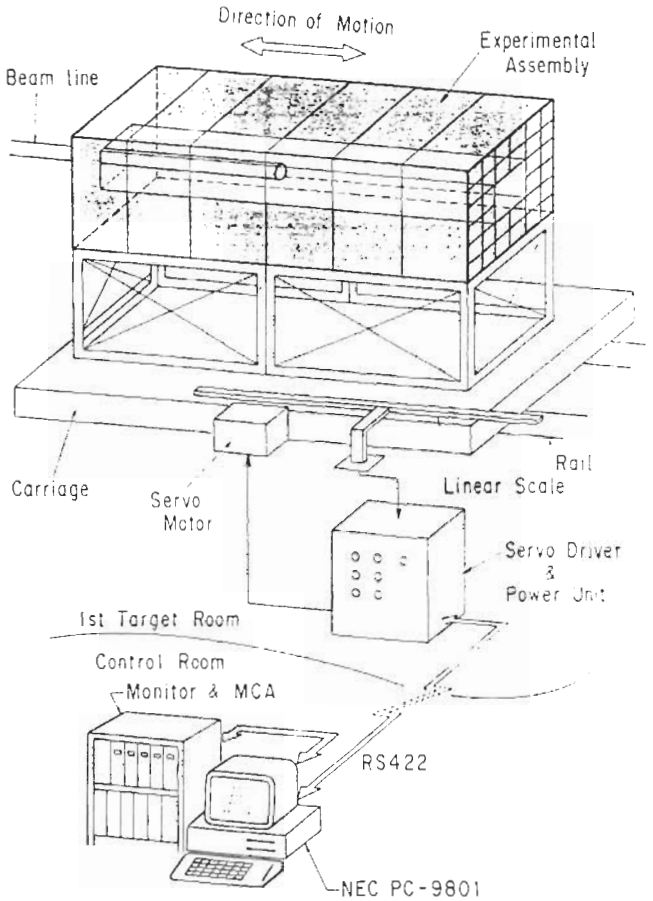

Fig. 1. The basic idea of the pseudoline source devices.

tube target assembly, a large movable deck, a pseudocylindrical annular blanket assembly, a controlled servomotor drive system, a position sensor, a neutron-monitoring system, and a managing computer. The long tube target assembly and the movable deck were installed in the larger irradiation room in the FNS facility. The room is 15 m square and 9 m high, and the floor is made by steel grating at a height from the base floor of 3 m, as shown in Fig. 2. The target motion inside the annular blanket needed to be accurately controlled to trace its central axis and to keep symmetry. Also, the requirements for moving speed and step motion mentioned earlier were reflected in the experimental system design.

The deck was designed to hold heavy material equipment, and its rails and wheel system were installed very carefully to ensure accurate linear motion. Two carriage decks were combined into one large deck 3.4 m wide and 4 m long to accommodate the annular test blanket assembly. Each deck had its own servomotor and was able to carry a weight up to 20 t. Four rails were installed and adjusted to keep the horizontal level within a 1-mm difference even if a 10-t duty was loaded. The target position was settled accurately by a laser transit, and the outer rails were aligned to the target straight and parallel to guide the wheels of the carriage deck. The deviations in both the horizontal and the vertical directions during motion were confirmed to be <1 mm over a 2-m stroke. By splitting the two decks, one could have easy access to the inner part of the annular test blanket whenever a change of assembly would be necessary. Figure 3 shows the arrangement that used the movable carriage deck for the line source with the blanket assembly to perform the annular blanket experiment.[9]

The deck motion was controlled by servomotor with the feedback from the position data measured by a 2.4-m-long linear scale with optical scale reading. The motor-driving system was controlled by a personal computer (NEC-9801DS) located in the measurement room far from the irradiation room through the RS-422 data bus line. A voltage drop type of current control was used for the servomotor power supply instead of a power supply with switching regulator elements because switching regulator noise would affect the measurements of the detector signal. The moving speed was determined by the setup of a stepping motor drive and adjusted to 6.1 mm/s for a normal speed. This speed is higher than the minimum requirement of 1.2 mm/s described previously.

In the stepwise mode, measurements are performed intermittently for a selected time interval (e.g., 1000 s) at equispaced points (e.g., 100 mm) over a 2-m length. The detector signals are collected during the stay of the source at each selected position and stopped during motion to the next position. The sequence of data acquisition and carriage deck control is programmed on a personal computer in connection with multichannel analyzer (MCA) and scaler (pulse counter) systems. This mode is suitable for on-line measurement techniques with higher detection efficiency such as NE-213 and Li-glass scintillators and proton-recoil gas proportional counters. This scheme can also provide the source positionwise data of the neutron response, corresponding to the importance (adjoint flux) distribution for a detector location along the line source. The measured data at each source position are normalized by the neutron emission yield calculated from the neutron monitor data taken synchronously.

In the continuous mode, the test blanket repeats the forth and back motions at a constant speed. For example, one cycle of motion takes 11 min with a speed of 6.1 mm/s. The obtained data are normalized by the total neutron emission yield, which is obtained from the integration of data periodically sampled by a neutron monitor during the whole continuous irradiation cycles. This mode is applied to passive measurement techniques such as activation foil, thermoluminescence dosimeter, and tritium production measurement by the liquid scintillation counting method with a lithium oxide (Li_2O) pellet. These passive methods require high neutron fluence and long irradiation time, so the stepwise mode is not practical in this case.

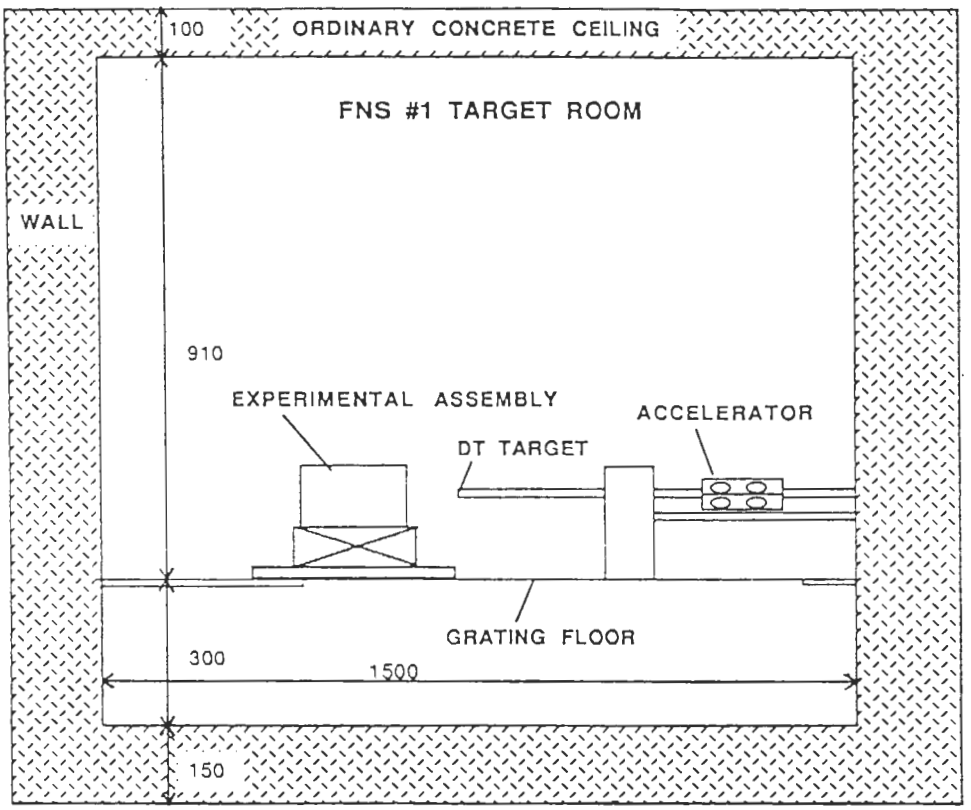

Fig. 2. Vertical cross section of irradiation room.

II.C. Long Tube Neutron Target and Neutron Monitor

The most important requirement of the neutron target is that the neutron emission not be influenced by the target structure. The target structure material should be light and thin to avoid neutron spectrum deformation due to neutron scattering. This requirement has not been ensured by the other design; for example, the large size of the elongated target proposed for FRBF[4] must have the disadvantage of a complex and heavy structure to ensure vacuum tightness, heat removal, and mechanical strength. Figure 4 shows the newly designed long tube water-cooled target assembly with a cup-shaped tritium metal target and a 2.3-m-long drift tube. The target assembly was made of Type 304 stainless steel and positioned without any support stands over 2 m. Steel wire was used to help sustain the whole weight of the assembly by a single side support, as shown in Fig. 3. The azimuthal symmetry was kept by a cylindrical shape, and the size was small enough to insert the assembly into the annular blanket.

Fig. 3. Test annular blanket assembly made of Li_2O and lithium carbonate on the movable deck and the long tube target.

The cup-shaped metal target assembly was designed to reduce the scattered neutrons by keeping the flange apart from the neutron production point and was made of thin stainless steel and copper. The cup-shaped part was insulated electrically to enable measurement of the beam current. The tritium was adsorbed in the ~4-μm titanium layer deposited on the bottom of the 1-mm-thick copper target backing with a cup shape. The total amount of tritium was ~370 GBq (10 Ci). The outside of the copper backing was cooled by a 1-mm-thick water layer covered by a 1-mm-thick stainless steel water jacket. The water flow line was bent backward to keep

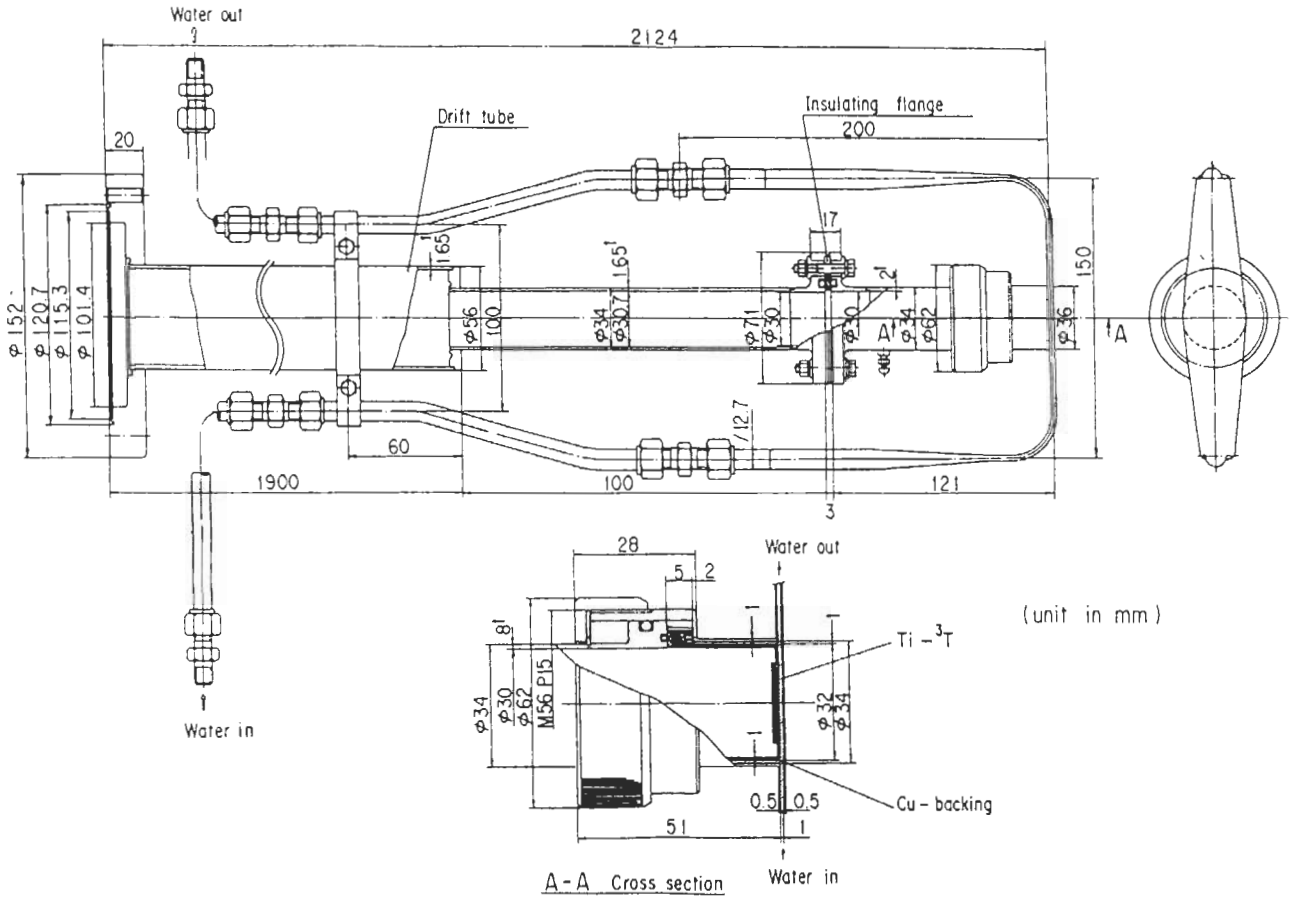

Fig. 4. Cross section of long tube water-cooled target assembly.

the size small so as to insert it into the inner cavity of the test blanket. The deuteron beam current could be controlled from 0.1 μA to 2 mA according to the type of measurement. The acceleration voltage was 350 kV. The position of the beam spot on the target surface was monitored by temperature distribution with an infrared thermal image measurement system to keep the beam spot at the center position. Keeping the beam position at the center is very important to achieve symmetry of the annular blanket system and accuracy of the distance between the source and the measuring positions.

The neutron production rate was monitored by detecting alpha particles emitted from the tritium-titanium layer associated with the D-T reaction. A small surface-barrier silicon-lithium detector with a 1-mm-diam collimator was located inside the beam drift tube 2.98 m from the target.[10] The low-current operation was adopted for the on-line detector measurements with high detection sensitivity. However, the counting rate of the neutron monitor was not enough because of the long distance from the distance from the target to the alpha-particle detector. Thus, the measurement time was determined by the statistics of the monitor counts, which required a longer measurement time at each source position. This was one of the reasons why the stepwise mode was chosen for the on-line measurement.

The alpha-particle counts were recorded on the computer every 10 s for the continuous mode and at every step for the stepwise mode. For the continuous mode, the source position data were also recorded at the same time. Figure 5 shows the time-dependent neutron yield and carriage deck position obtained from this system. Figure 5 indicates that the neutrons were generated stably and the carriage deck moved with a constant speed. At the turning points, however, the speed did not ideally change from forward to backward; it gradually slowed down and speeded up at both ends. The slowing down of the moving speed at both ends increased the staying time of the carriage deck and made the neutron intensity higher at both ends. For the continuous mode, this end effect was considered in the correction factor for the activation foil detector, as described in Sec. III.A.2.

III. CHARACTERISTICS OF LINE SOURCE

An accelerator-based D-T reaction neutron source has angular dependence of energy spectrum and the

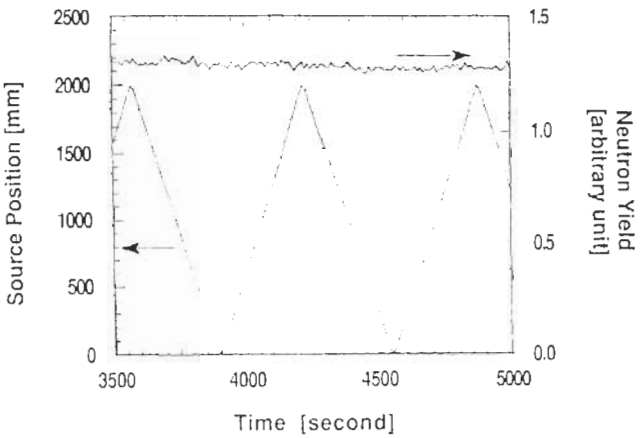

Fig. 5. Time dependence of neutron emission yield and carriage deck position.

yield as determined by reaction kinematics. In addition, the realistic tritium-titanium metal target has deformed emission characteristics of energy and angular distributions due to neutron scattering on the target structure. Previous research on neutron source characteristics of the accelerator D-T source[11] proved that a Monte Carlo calculation can reproduce well the measured neutron spectrum and angular distribution. Thus, one can expect that the spectrum and angular yield can be provided by a Monte Carlo calculation with good accuracy even for the current line source. However, because this line source is produced in a more complicated way, the results of the Monte Carlo calculation should be checked with an experiment. For this purpose, measurements of the neutron flux distribution around the line source were performed and compared with the Monte Carlo calculation.

III.A. Experiment of Line Source Characteristics

The continuous mode has nonuniformity of the neutron intensity distribution at both ends while the stepwise mode is not practical for activation detectors with shorter lifetimes. The detector responses around the line source with both operation modes are directly connected with practical source characteristics because those responses for this line source are measured in neutronics experiments. A source model used in the calculational analysis for such experiments should be able to explain the detector response for the bare line source. Thus, measurements of the source characteristics were performed for both operation modes to test the source model.[12]

III.A.1. Measurement for Stepwise Mode

The source characteristics for the stepwise mode were measured by using a small sphere NE-213 scintillation detector.[13] The measurement was performed along three different lines 4 m long and parallel to the line source. The distances of the lines were 200, 400, and 600 mm from the source axis. Figure 6 shows a photograph of the experimental setup of the detector and the carriage deck. The step of the deck motion was chosen at a 50-mm equiinterval. The neutron flux distributions around the line source were composed by superposition of the data obtained at every source position with numerical processing. The data of a total of 81 measuring points were taken for the distribution at each line along the source and at three different distances from the line source. For example, the superposition of the first 41 data points gave the neutron flux at the end of a 2-m-long line source. Then, the group of 41 data points for superposition was shifted by one data point, and that group corresponded to the flux data at the next mapping position of the line source.

The flux distributions at three distances were taken at the same time by three equivalent NE-213 detectors. By the NE-213 detectors, only a neutron flux above 10 MeV was obtained using the spectrum weighting function method,[14] which converted directly from the recoiled proton spectrum to the integral neutron flux, to process a large number of data in a shorter time. The data of 81 positions at each distance are shown in Fig. 7. A deformed distribution was seen just beside the target. This was caused by the deformation at ~90 deg in angular neutron emission yield from the target due to scattering by the target structure. The deformation was wider for the distribution at a longer distance because the same solid angle covered a larger area at a far position.

These measured data were summed up to be superposed in space: The 81 position data for the point source were reduced to 41 position data for the line source; i.e., the flux distribution over 4 m around the point neutron source was converted to the superposed

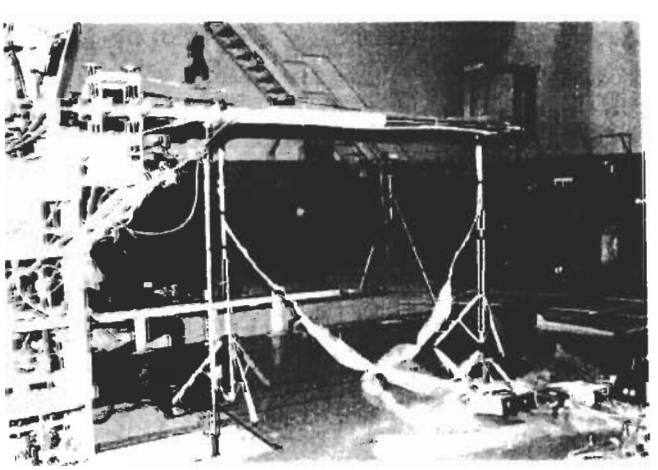

Fig. 6. Long tube target assembly and setup of the NE-213 detector for measurement of the source positionwise neutron flux.

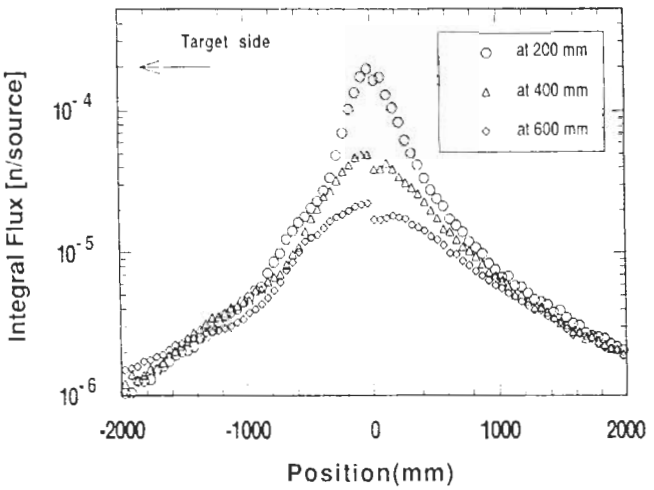

Fig. 7. The source positionwise integrated neutron flux measured by the NE-21 detector.

flux distribution over 2 m around the 2-m line source. For an ideally isotropic and nondisturbed line source, the neutron flux distribution is calculated analytically by the following equation:

$$\Phi = \frac{\sigma}{4\pi r} \cdot \left(\tan^{-1} \frac{L-a}{r} + \tan^{-1} \frac{L+a}{r} \right) \quad (\mathrm{n/cm^2}) , \tag{1}$$

where

σ = linear density of the neutron source intensity (n/cm)

L = half of line source length

a = distance from the center

r = vertical distance from the line source, as illustrated in Fig. 8.

Figure 9 shows the neutron flux distribution above 10 MeV superposed by the measured data with the NE-213 detectors and the distribution calculated by Eq. (1). The measured distributions were smaller than the calculated ones by 10 to 15% because the loss of the angular neutron emission at 90 deg also produced anisotropy of the linear density of the source, and then the total number of emitted neutrons above 10 MeV became smaller. In symmetrical comparison, the neutron flux at the forward of the target was larger in the measured distribution than at the backward. This was caused by anisotropy of neutron emission due to kinematics; i.e., in the reaction kinematics for a 350-keV deuteron, the forward neutron emission was ~8% larger than at 90 deg. Nevertheless, the relative distribution agreed well within 5%, and the distribution at the mid-region was very smooth and flat, which ensured that the current pseudoline source could represent a similar characteristic of an ideal line source.

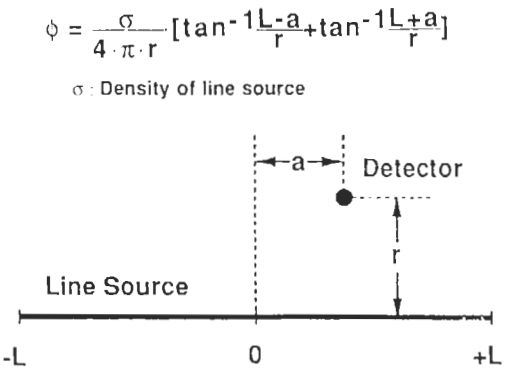

Fig. 8. Neutron flux calculation around an ideal line source.

To answer the question of how many points are enough to simulate a line source by the stepwise mode, we changed the number of points to be superposed. This examination gave the minimum step necessary to simulate a line source. The discussion in Ref. 8 suggests that a 125-mm interval, i.e., 16 steps, is necessary for such a minimum requirement. We compared four types of equiintervals: 50, 100, 200, and 400 mm; the distributions with 50-mm spatial resolution were obtained from 41, 21, 11, and 6 data points for each position. Figure 10 shows a comparison of the superposed flux distribution with different sets of data points 200 mm from the line source. The coarser step interval shows an oscillation and a deformation compared with the reference distribution obtained with 50-mm spatial resolution. The range of oscillation for the 100-mm interval agreed well with the 50-mm interval case within 3%.

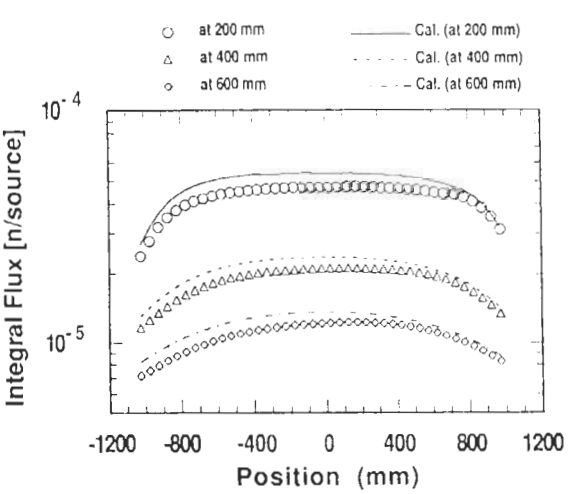

Fig. 9. Comparison of the measured flux distribution around the line source with the calculation for an ideal line source.

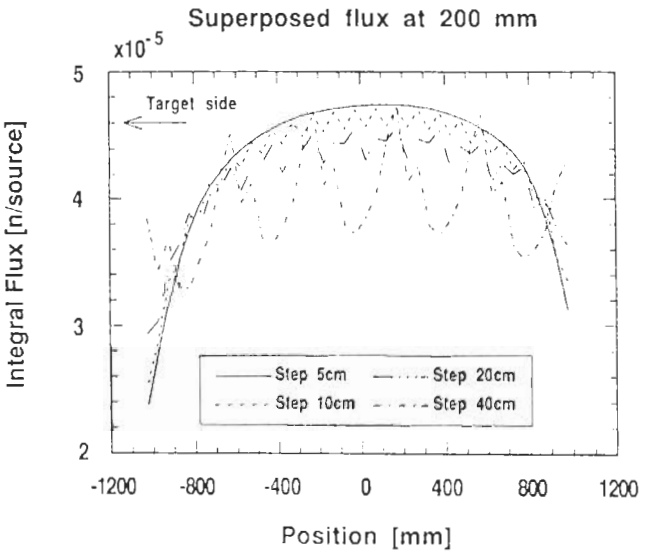

Fig. 10. Comparison of the superposed flux from the data at different intervals.

Considering the experimental accuracy of the on-line detectors, we found that the 100-mm interval case was enough to simulate the line source.

III.A.2. Measurement for Continuous Mode

Although the line source is simulated by time averaging in the continuous mode, the nuclear response that has a time-dependent property can be applied approximately with a correction. As discussed in Ref. 12, the time dependence of nuclear responses can be corrected by using time-dependent source position and neutron yield data if one assumes that only an uncollided flux distribution is associated with the response. For an activation foil detector at each position, the neutron flux varies by $1/r^2$ dependence with the source position moving along the pseudoline source, i.e., with the time past from the beginning of irradiation. This kind of time-dependent nuclear response is usually taken into account in activation reaction measurement by considering the irradiation history together with the decay property of activity. For the line source, this type of correction can be made by disassembling the line source to the distributed sources sampled every 10 s by a neutron-monitoring system. The real irradiation is reconstructed by individual irradiation from each registered source. Then, the correction factor of the current measurement is obtained from the following ratio; i.e., the correction PF for each point source is obtained as

$$PF = \sum_{j=1}^{M} \left\{ \frac{S_j}{4\pi r_j^2} \cdot [1 - \exp(-\lambda \cdot \Delta t)] \times \exp[-\lambda \cdot (M - j) \cdot \Delta t] \right\} , \quad (2)$$

where

S_j = source yield sampled by j'th monitor data at each source position r_j

$[1 - \exp(-\lambda \cdot \Delta t)]$ = correction for decay time λ during irradiation time Δt

$\exp[-\lambda \cdot (M - j) \cdot \Delta t]$ = correction for decay for the rest time $(M - j) \cdot \Delta t$ by the end of whole irradiation time by the continuous line source mode.

On the other hand, the correction LF for an ideal line source is written as

$$LF = \left(\sum_{j=1}^{M} \frac{S_j}{2 \cdot L \cdot M} \right) \cdot \frac{1}{4 \cdot \pi \cdot r} \times \left(\tan^{-1} \frac{L - a}{R} + \tan^{-1} \frac{L + a}{R} \right) \times [1 - \exp(-\lambda \cdot t_r)] , \quad (3)$$

where

$\left(\sum_{j=1}^{M} \frac{S_j}{2 \cdot L \cdot M} \right)$ = line source density σ (L = half-length of the line source, M = number of sample points)

$\frac{1}{4 \cdot \pi \cdot r} \cdot \left(\tan^{-1} \frac{L - a}{R} + \tan^{-1} \frac{L + a}{R} \right)$ = expected flux for ideal line source with the definition as given in Eq. (1)

$[1 - \exp(-\lambda \cdot t_r)]$ = decay correction during the whole irradiation time t_r.

Then the correction F for the pseudoline source by the continuous mode is obtained from the ratio of them:

$$F = \frac{LF(\textit{line source})}{PF(\textit{point source sum})} . \quad (4)$$

Finally, the reaction rate is obtained from the photon counts measured by a germanium detector as follows:

$$RR = \frac{\lambda \cdot C \cdot F}{\epsilon \cdot N \cdot B \cdot [1 - \exp(-\lambda \cdot \Delta t)] \cdot \exp(-\lambda \cdot t_c) \cdot [1 - \exp(\lambda \cdot t_m)]} , \quad (5)$$

where

C = count detected by a germanium detector

ϵ = efficiency of the germanium detector

N = number of nuclei in the foil

B = branching ratio for the decay of interest

t_c = cooling time from end of the irradiation to the measurement

t_m = measuring time for gamma emission.

Assuming that the carriage deck moves with a constant speed of 6.1 mm/s, we find that the estimated correction factor for a $^{115}\mathrm{In}(n,n')^{115m}\mathrm{In}$ reaction ($T_{1/2}$ = 4.49 h) with 10-h irradiation is 1.09 and the largest correction is due to a decrease of the source neutron yield caused by depression of the amount of tritium in the target. The correction factors are calculated with the record of neutron and position monitors during irradiation and applied to data reduction. Figure 11 shows typical samples of the calculated correction factors for three reactions with decay times of 4.5 h to 10 days. The correction factors decreased by 8% at both turning points where the moving speed of the carriage deck slowed down. The factor for the $^{115}\mathrm{In}(n,n')^{115m}\mathrm{In}$ reaction case with a shorter decay time was ~8% while the longer decay cases were <4%.

Table I summarizes the activation reactions used in the measurement of the reaction rate distribution around the line source. Foils were located 219 mm from the line source with 200-mm intervals. These foils were packed and put onto nylon strings stretched by a support on the carriage deck. The irradiation was performed for 10 h, and the neutron yield obtained was 7.8×10^{15} n/s in total emission. The measured results of the reaction rates 219 mm from the line source are summarized in Table II and shown in Fig. 12. The distribution of the threshold reactions was similar to that calculated for an ideal line source while the $^{197}\mathrm{Au}(n,\gamma)^{198}\mathrm{Au}$ reaction was completely flat over the source length. Figure 13 plots the ratios of the reaction rates to their central values to see the symmetry of distribution. One can see that the forward result in the $^{58}\mathrm{Ni}(n,2n)^{57}\mathrm{Ni}$ reaction

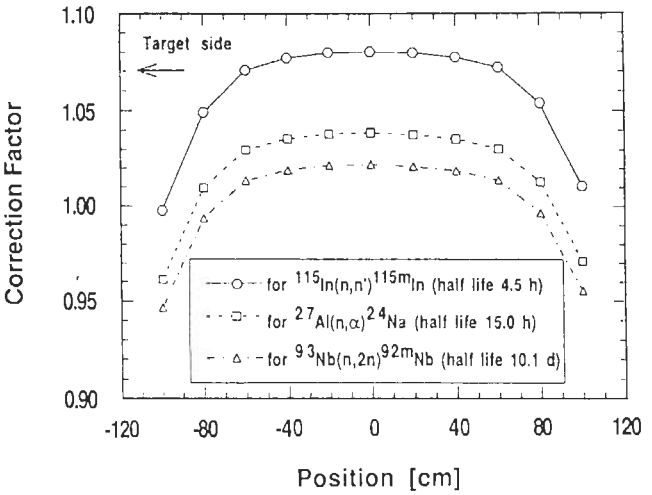

Fig. 11. Correction factors for the activation reaction with three different decay times.

TABLE I

Dosimetry Reactions Used in the Source Characteristics Experiments

Reaction	Half-Life	Abundance (%)	Gamma-Ray Energy (keV)	Gamma-Ray Branching (%)	Threshold Energy (MeV)	Typical Foil Size (mm)
$^{27}\mathrm{Al}(n,\alpha)^{24}\mathrm{Na}$	15.02 h	100.0	1368.6	100.0	5	15 diam × 1
$^{nat}\mathrm{Ti}(n,x)^{46}\mathrm{Sc}$	83.83 days	100.0	889.3	99.98	4	20 diam × 1
$^{nat}\mathrm{Ti}(n,x)^{47}\mathrm{Sc}$	3.341 days	100.0	159.4	68.0	1.5	20 diam × 1
$^{nat}\mathrm{Ti}(n,x)^{48}\mathrm{Sc}$	1.821 days	100.0	983.5	100.0	5	20 diam × 1
$\mathrm{Fe}(n,x)^{56}\mathrm{Mn}$	2.579 h	100.0	846.8	98.9	---	10 diam × 1
$^{54}\mathrm{Fe}(n,p)^{54}\mathrm{Mn}$	312.2 days	5.8	834.8	99.98	2	10 diam × 1
$^{58}\mathrm{Ni}(n,p)^{58}\mathrm{Co}$	70.92 days	68.26	810.8	99.5	2	15 diam × 1
$^{58}\mathrm{Ni}(n,2n)^{57}\mathrm{Ni}$	1.503 days	68.27	1377.6	77.9	12.5	15 diam × 1
$^{59}\mathrm{Co}(n,\alpha)^{56}\mathrm{Mn}$	2.579 h	100.0	846.8	98.9	6	10 diam × 1
$^{64}\mathrm{Zn}(n,p)^{64}\mathrm{Cu}$	12.70 h	48.6	511.0	74.2	1.5	20 diam × 1
$^{90}\mathrm{Zr}(n,2n)^{89}\mathrm{Zr}$	3.268 days	51.45	909.2	99.01	12	20 diam × 1
$^{93}\mathrm{Nb}(n,2n)^{92m}\mathrm{Nb}$	10.15 days	100.0	934.5	99.0	9	20 diam × 1
$^{115}\mathrm{In}(n,n')^{115m}\mathrm{In}$	4.486 h	95.7	336.3	45.8	0.34	10 × 10 × 1
$^{197}\mathrm{Au}(n,\gamma)^{198}\mathrm{Au}$	2.694 days	100.0	411.8	95.5	---	10 × 10 × 0.001

TABLE II

Reaction Rate Distributions Along the Line Source at a Distance of 219 mm from the Line Source Without Blanket*

Distance from Center of Assembly (mm)	$^{127}Al(n,\alpha)^{24}Na$	$Ti(n,x)^{46}Sc$	$Ti(n,x)^{47}Sc$	$Ti(n,x)^{48}Sc$	$^{54}Fe(n,p)^{54}Mn$
−1000.0[a]	2.943E−30(3.2)[b]	3.707E−30(4.2)	3.870E−31(3.6)	1.279E−30(3.3)	9.347E−30(6.6)
−800.0	4.497E−30(3.1)	---	---	---	---
−600.0	5.066E−30(3.1)	---	---	---	---
−400.0	5.375E−30(3.1)	6.917E−30(4.3)	8.554E−31(3.5)	2.458E−30(3.2)	1.643E−29(6.1)
−200.0	5.584E−30(3.1)	---	---	---	---
0.0	5.587E−30(3.1)	7.019E−30(3.9)	9.255E−31(3.5)	2.587E−30(3.2)	1.690E−29(6.1)
200.0	5.573E−30(3.1)	---	---	---	---
400.0	5.439E−30(3.1)	6.961E−30(3.8)	9.120E−31(3.5)	2.518E−30(3.2)	1.651E−29(6.2)
600.0	5.084E−30(3.1)	---	---	---	---
800.0	4.603E−30(3.1)	---	---	---	---
1000.0	2.998E−30(3.1)	3.819E−30(4.1)	5.691E−31(3.5)	1.442E−30(3.3)	8.937E−30(6.5)

Distance from Center of Assembly (mm)	$Fe(n,x)^{56}Mn$	$^{59}Co(n,\alpha)^{56}Mn$	$^{58}Ni(n,2n)^{57}Ni$	$^{58}Ni(n,p)^{58}Co$	$^{64}Zn(n,p)^{64}Cu$
−1000.0	2.596E−30(3.1)	---	3.621E−31(4.0)	9.566E−30(3.3)	4.303E−30(3.1)
−800.0	---	---	---	---	---
−600.0	---	---	---	---	---
−400.0	4.910E−30(3.1)	1.356E−30(3.1)	1.064E−30(3.8)	1.625E−29(3.3)	7.608E−30(3.0)
−200.0	---	---	---	---	---
0.0	5.286E−30(3.1)	1.407E−30(3.1)	1.173E−30(3.8)	1.672E−29(3.3)	7.809E−30(3.0)
200.0	---	---	---	---	---
400.0	5.069E−30(3.1)	1.389E−30(3.1)	1.227E−30(3.8)	1.622E−29(3.3)	7.565E−30(3.0)
600.0	---	---	---	---	---
800.0	---	---	---	---	---
1000.0	2.874E−30(3.1)	---	8.837E−31(3.8)	8.694E−30(3.3)	3.806E−30(3.1)

Distance from Center of Assembly (mm)	$^{90}Zr(n,2n)^{89}Zr$	$^{93}Nb(n,2n)^{92m}Nb$	$^{115}In(n,n')^{115m}In$	$^{197}Au(n,\gamma)^{198}Au$	
−1000.0	1.117E−29(3.1)	1.052E−29(2.8)	2.196E−30(3.5)	2.212E−29(6.5)	
−800.0	---	1.670E−29(2.9)	3.205E−30(3.5)	2.787E−29(7.9)	
−600.0	---	1.969E−29(2.9)	3.701E−30(3.4)	2.984E−29(8.1)	
−400.0	2.712E−29(3.0)	2.057E−29(2.9)	3.785E−30(3.4)	2.631E−29(7.9)	
−200.0	---	2.138E−29(2.9)	3.989E−30(3.4)	2.442E−29(10.6)	
0.0	2.960E−29(3.0)	2.185E−29(2.8)	4.054E−30(3.4)	2.797E−29(7.5)	
200.0	---	2.142E−29(2.9)	3.894E−30(3.4)	2.511E−29(10.0)	
400.0	2.925E−29(3.0)	2.105E−29(2.9)	3.904E−30(3.5)	2.016E−29(12.1)	
600.0	---	2.044E−29(2.9)	3.597E−30(3.4)	2.517E−29(7.5)	
800.0	---	1.832E−29(2.9)	3.182E−30(3.5)	2.500E−29(12.6)	
1000.0	2.020E−29(3.1)	1.292E−29(2.8)	2.074E−30(3.5)	2.644E−29(11.0)	

*Distance is measured from the beam drift tube side.
[a]This is 20 mm from the front end of the assembly.
[b]Read as 2.943×10^{-30} (reaction/total source neutron) with 3.2% relative error.

was larger than the backward. This was because the energy of the neutrons emitted forward from the target was higher than that of the backward and the $^{58}Ni(n,2n)^{57}Ni$ cross section for the higher energy neutrons was larger. Because the reactions with lower thresholds are rather symmetric, the effect of anisotropy on neutron emission yield by kinematics is not so large.

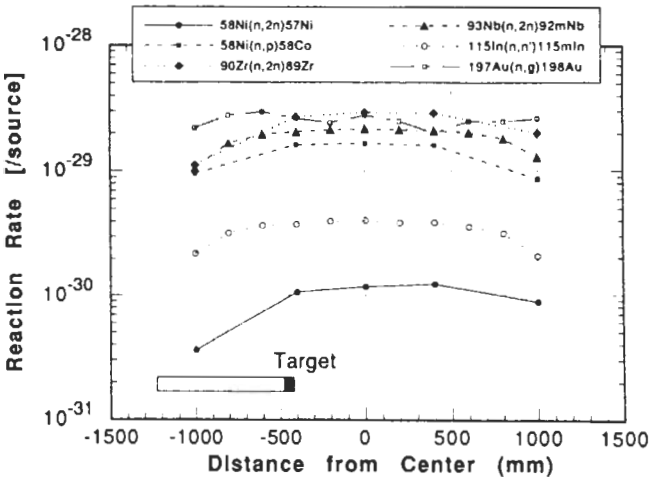

Fig. 12. Reaction rate distributions measured around the line source.

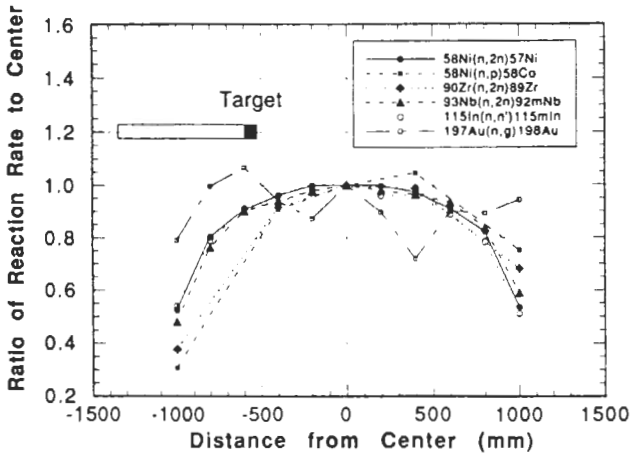

Fig. 13. Ratios of the reaction rates to those at the center.

III.B. Calculation of Line Source Characteristics

III.B.1. Monte Carlo Calculation of Long Tube Target

Because the current pseudoline source was approximated by superposition by point sources from each position during motion, the line source performance was based on the neutron emission characteristics of the long tube target. In the computational analysis for the successive experiment, the line source was generated by the distributed source for the deterministic code. Thus, the calculation of the neutron emission characteristics was performed for the stationary long tube target.

The neutron production reaction, the deuteron deceleration process in the tritium-titanium layer, and the neutron scattering were calculated by the external subroutine of the MORSE-DD Monte Carlo code[15] that uses a library based on the JENDL-3 nuclear data file.[16] The calculation model simulated completely the components around the neutron emission point. The validity of this model was confirmed by comparison of the calculated spectrum with the measured one performed by the time-of-flight technique in the previous experiments.[11] The current calculation differed from the previous one only in the target structure so that it was expected to have similar accuracy. Because the source neutrons came from the superposed line source with different emission angles to the detector, the angular distribution was needed for fine calculation. To calculate the fine angular distribution in the Monte Carlo calculation, we placed the point estimators with 5-deg intervals on a horizontal plane and 15-deg intervals on a vertical plane at a distance 100 mm from the neutron emission point. When we set the detector 400 mm from the line source (at the middle of the test blanket), the source step of 50 mm corresponded to the angle difference of 7 deg for neutron emission. Hence, the angle interval of 5 deg was adopted in the source characteristic calculation by the Monte Carlo code.

Figure 14 shows the calculated angular dependence of neutron emission for the vertical and the horizontal directions. Deformation of ~20% existed at 90 and ~140 deg. The former was due to the target backing whose plane was parallel to the 90 deg and made the longest path through the backing material for the

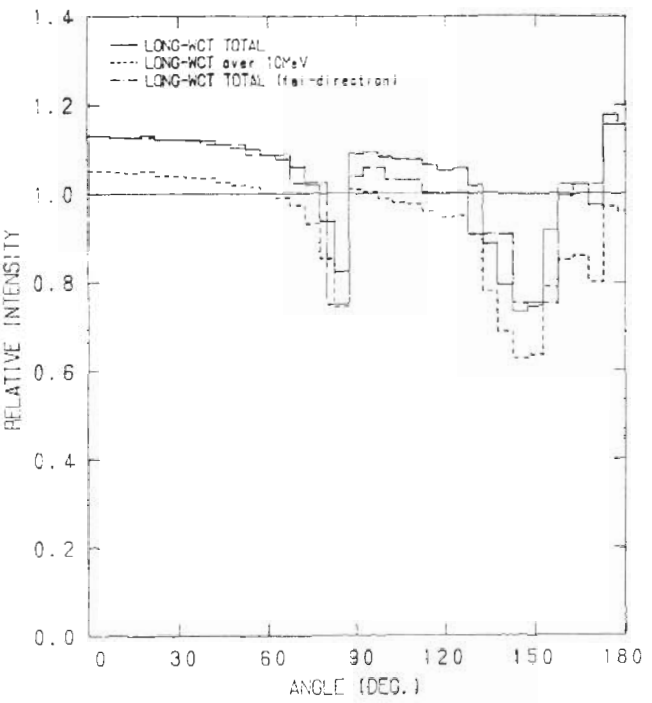

Fig. 14. Angular dependence of neutron emission yield obtained by Monte Carlo calculation. (Water-cooled target is designated by WCT.)

neutrons. The latter was caused by the flange structure of the target assembly. Because this target was specially designed as a cup shape, the dip at 90 deg was very sharp. Nevertheless, the 90-deg direction must be considered in an annular blanket experiment that uses the current line source system. Figure 14 also shows anisotropy of angular emission yields due to kinematics; the forward emission was larger than the backward. Figure 15 shows the calculated neutron energy spectra for three directions. By kinematics relation at 350-keV deuteron energy, the forward energy was 14.8 MeV, and the backward was 13.4 MeV. These effects of the neutron emission profile were clearly observed in the measured source characteristics of the line source.

III.B.2. Reliability of Calculated Line Source Model

Using the foregoing results for the long tube point source, we calculated the neutron flux distributions around the line source by the FNSUNCL code,[17] which was modified from the GRTUNCL code. The GRTUNCL code calculates the first collision source from a point source and provides an input source distribution for the next step calculation by using the DOT3.5 two-dimensional discrete ordinates transport code.[18] On the other hand, FNSUNCL can calculate the first collision source from every point source distributed along the line and sum up the contributions from all point sources taking account of the angular distributions of both the energy spectrum and the emission yield. To calculate the neutron flux distribution around this line source, we chose 40 points to be distributed on the source line with 50-mm intervals, based on the discussion of superposition. Thirty-seven neutron energy spectra from 0 to 180 deg with a 5-deg step calculated by the Monte Carlo code were generated at each source position.

Using the calculated neutron angular emission yield, we reduced the flux distributions along the target assembly axis corresponding to the measured distributions given in Fig. 7 and compared them with the measurement. Figure 16 shows the flux distributions above 10 MeV around a long tube target for both the calculation and the measurement. The results showed excellent agreement with each other, except for the backward distribution, which showed disagreement due to an insufficient model for the beam drift tube. However, the good agreement in the main part of the distribution enables one to be able to use the calculated neutron source as the initial source condition for an analysis of a neutronics experiment that uses this line source.

The calculated reaction rates around the pseudoline source were also compared with the measured results of the activation reaction with the continuous mode. The calculated-to-the-measured-value ratios (C/E) are shown in Figs. 17, 18, and 19 for various threshold reactions. The reaction cross-section data used in the calculation were based on Ref. 16 for the $(n,2n)$ reactions and on ENDF/B-IV for the others. For all the reactions, the tendency of the C/Es was very consistent with the ratios of the cross sections measured at FNS reported in Ref. 16 to both JENDL-3 and ENDF/B-IV. The (n,p) reactions of ^{64}Zn and ^{58}Ni showed large C/Es, and those reaction cross sections of ENDF/B-IV were larger. Because an agreement was within $\pm 5\%$ for the calculation using the measured $(n,2n)$ reaction cross sections, the accuracy of the calculation by

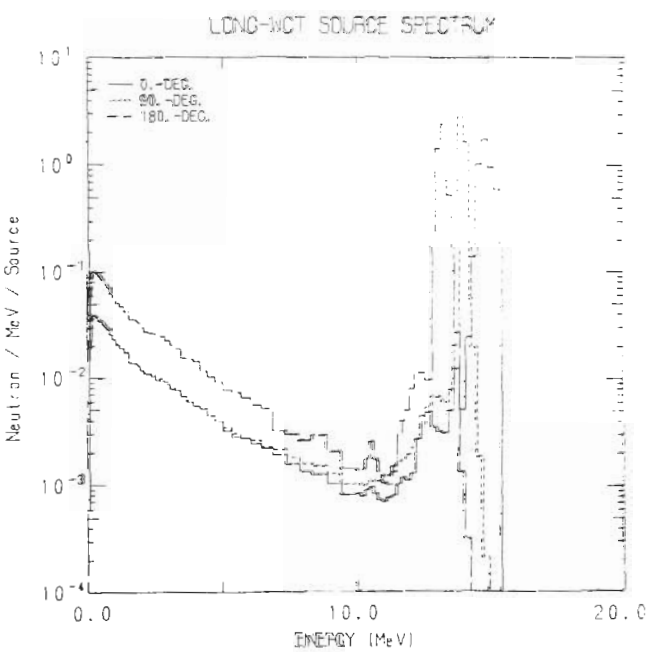

Fig. 15. Calculated neutron energy spectra at three emission angles.

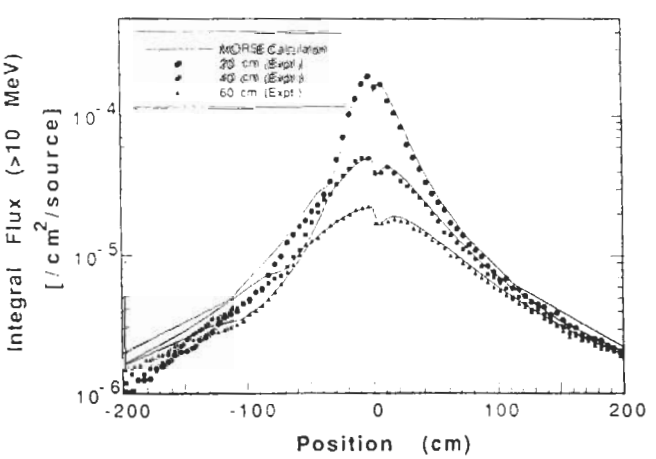

Fig. 16. Comparison of the measured neutron flux distributions to the calculated ones around the fixed point source of the long tube target.

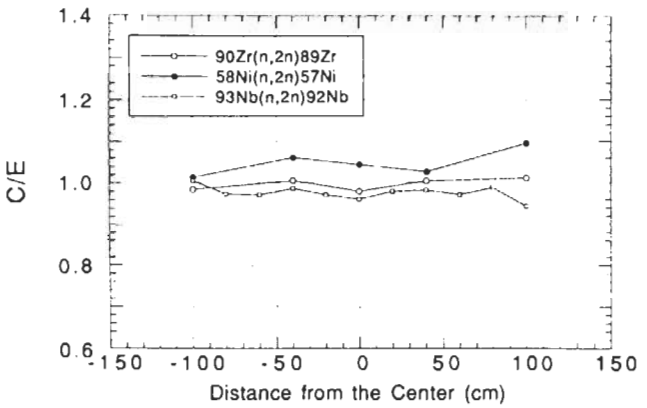

Fig. 17. Ratios of C/E for the $(n,2n)$ reactions.

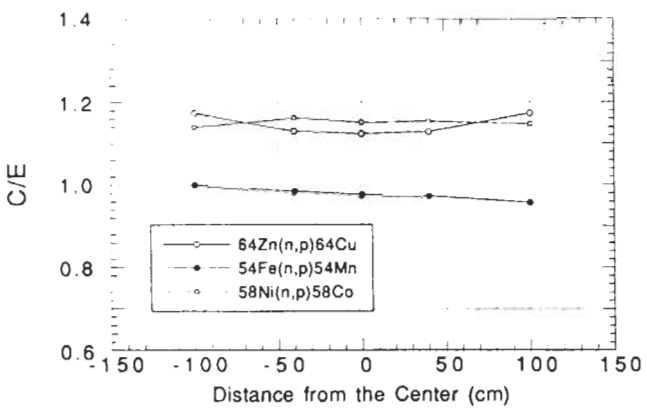

Fig. 18. Ratios of C/E for the (n,p) reactions.

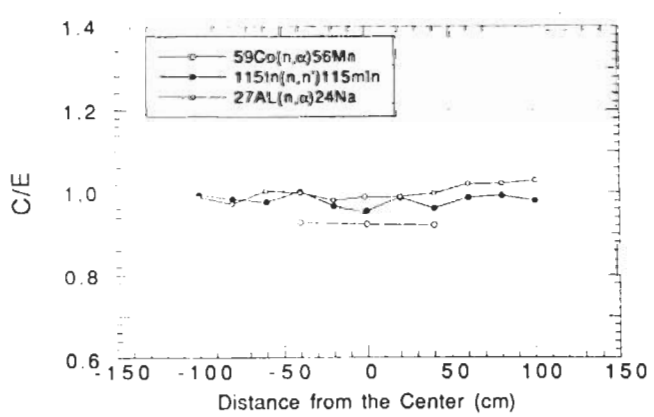

Fig. 19. Ratios of C/E for the (n,n') and (n,α) reactions.

the Monte Carlo code and FNSUNCL was also expected to be within a few percent. This proved again that the calculated neutron energy spectra and the emission probability could be used as the initial source condition of the successive calculations for an analysis of an experiment that uses this line source. Also, the distributed source with the interval of 50 mm was confirmed to be equivalent to the line source with the continuous mode, and the correction method for activation decay was valid.

IV. CONCLUDING REMARKS

A pseudoline D-T neutron source system was successfully developed to simulate a distributed source relevant to a tokamak D-T–fueled fusion reactor. The line source system consisted of an automatic controlled moving carriage deck, a long drift tube, a water-cooled target assembly, and a synchronized data acquisition system. The operation could be performed in two ways: in the stepwise and in the continuous-moving modes. The neutron flux distributions for both operation conditions were measured around the target. The source intensity was normalized by the counts of alpha particles emitted from the D-T reaction. The obtained neutron field around the line source was very smooth and flat in the central region over 1 m.

The energy spectrum and the angular emission yield of the neutrons emitted from the long tube D-T target were calculated by the Monte Carlo code. These data were confirmed by comparison with the experiments of the source characteristic and validated for use as the initial source condition for a calculational analysis of experiments to be performed by using this line source system.

This line source system provides a powerful tool for benchmark experiments and opens a new experimental area that examines the overall performance of the design codes, especially for the engineering confirmation containing the complexity of prototypical configurations.

ACKNOWLEDGMENTS

The authors thank the members of the FNS operation group for their excellent operation and assistance with the experiment. The U.S. contributions to the joint collaborative program were supported by the U.S. DOE Office of Fusion Energy.

REFERENCES

1. S. SAHIN and A. KUMAR, "Neutronics Analysis of Deuterium-Tritium-Driven Experimental Hybrid Blankets," *Fusion Technol.*, **6**, 97 (1984).

2. S. SAHIN and T. A. AL-KUSAYER, "Conceptual Design Studies of a Cylindrical Experimental ThO_2 Hybrid Blanket with (D,D) Driver," *Atomkernenergie*, **47**, 259 (1985).

3. S. SAHIN, T. A. AL-KUSAYER, and M. A. RAOOF, "Preliminary Design Studies of a Cylindrical Experimental Hybrid Blanket with Deuterium-Tritium Driver," *Fusion Technol.*, **10**, 84 (1986).

4. D. E. BELLER, K. O. OTT, and W. K. TERRY, "Conceptual Design and Neutronics Analyses of a Fusion Reactor Blanket Simulation Facility," *Nucl. Sci. Eng.*, **97**, 175 (1987).

5. D. L. SMITH et al., "Blanket Comparison and Selection Study, Final Report," ANL/FPP-84-1, Argonne National Laboratory (1984).

6. T. NAKAMURA and M. A. ABDOU, "Summary of Recent Results from the JAERI/U.S. Fusion Neutronics Phase I Experiments," *Fusion Technol.*, **10**, 541 (1986).

7. T. NAKAMURA, H. MAEKAWA, Y. IKEDA, and Y. OYAMA, "A D-T Neutron Source for Fusion Neutronics Experiments at the JAERI," *Proc. 7th Symp. (1983 Int.) Ion Sources and Ion-Assisted Technology (ISIAT'83)*, and *4th Int. Conf. Ion and Plasma-Assisted Techniques (IPAT'83)*, Kyoto, Japan, September 12–16, 1983, Institute of Electrical Engineers of Japan.

8. T. NAKAMURA et al., "A Line D-T Neutron Source Facility for Annular Blanket Experiment: Phase III of the JAERI/USDOE Collaborative Program on Fusion Neutronics," *Fusion Technol.*, **19**, 1873 (1991); see also M. Z. YOUSSEF, Y. WATANABE, A. KUMAR, Y. OYAMA, and K. KOSAKO, "Analysis for the Simulation of a Line Source by a 14 MeV Moving Point Source and Impact on Blanket Characteristics: The USDOE/JAERI Collaborative Program on Fusion Neutronics," *Fusion Technol.*, **19**, 1843 (1991).

9. C. KONNO et al., "Neutronics Integral Experiments of Annular Blanket System Simulating Tokamak Reactor Configuration," *Fusion Technol.*, **28**, 347 (1995).

10. H. MAEKAWA et al., "Neutron Yield Monitors for the Fusion Neutronics Source (FNS)," JAERI-M 84-193, Japan Atomic Energy Research Institute (1984).

11. Y. OYAMA, Y. IKEDA, T. MORI, M. NAKAGAWA, T. NAKAMURA, and H. MAEKAWA, "Neutron Field Characteristics in a Concrete Cavity Having a DT Neutron Source," *Fusion Technol.*, **10**, 585 (1986).

12. C. KONNO et al., "Measurements of the Source Term for Annular Blanket Experiment with a Line Source: Phase IIIA of the JAERI/USDOE Collaborative Program on Fusion Neutronics," *Fusion Technol.*, **19**, 1885 (1991).

13. Y. OYAMA, S. TANAKA, K. TSUDA, Y. IKEDA, and H. MAEKAWA, "A Small Spherical NE213 Scintillation Detector for Use in In-Assembly Fast Neutron Spectrum Measurement," *Nucl. Instrum. Methods*, **A256**, 333 (1987).

14. Y. OYAMA and K. SEKIYAMA, "Application of Spectrum Weighting Function Method to the Measurement of Fusion Nuclear Response with a Small NE213 Detector," Japan Atomic Energy Research Institute, Private Communication (1991).

15. M. NAKAGAWA and T. MORI, "MORSE-DD, A Monte Carlo Code Using Multigroup Double Differential Form Cross Sections," JAERI-M 84-126, Japan Atomic Energy Research Institute (1984).

16. K. SHIBATA et al., "Japanese Evaluated Nuclear Data Library, Version-3-JENDL-3-," JAERI 1319, Japan Atomic Energy Research Institute (1990).

17. K. KOSAKO, Sumitomo Atomic Energy Industries, "FNSUNCL," Private Communication (1990).

18. W. A. RHOADES and F. R. MYNETT, "The DOT-III Two-Dimensional Discrete Ordinate Transport Code," ORNL-TM-4280, Oak Ridge National Laboratory (1973).

Yukio Oyama (BS, physics, 1975; MS, nuclear physics, 1977; and Dr. Eng., 1989, Osaka University, Japan) is a principal scientist at the Japan Atomic Energy Research Institute (JAERI). He has worked in the area of fusion neutronics experiments since 1978. He is currently involved in intense and high-energy neutron source projects.

Chikara Konno (MS, physics, Kyoto University, Japan, 1985) is a research scientist in the Department of Reactor Engineering at JAERI. He has worked in the areas of fusion neutronics experiments, cross-section measurements, and neutron spectrum measurements using a proton-recoil counter.

Yujiro Ikeda (PhD, nuclear engineering, Nagoya University, Japan, 1981) is head of the Fusion Neutronics Laboratory in the Department of Reactor Engineering at JAERI. He has worked in the areas of fusion neutronics experiments, induced radioactivity experiment and analysis, direct nuclear heating measurements, activation cross-section measurements, and fusion dosimetry.

Kazuaki Kosako (BE, atomic engineering, Tokai University, Japan, 1984) has worked at Sumitomo Atomic Energy Industries since 1994. He worked in the Department of Reactor Engineering at JAERI from 1984 to 1992 where

he was involved mainly in fusion neutronics. He is currently interested in the area of radiation damage of materials.

Hiroshi Maekawa (BE, 1965; MS, 1967; and Dr. Eng., 1970, nuclear engineering, Tokyo Institute of Technology, Japan) is the deputy director of the Department of Reactor Engineering and the head of the Intense Neutron Source Laboratory at JAERI. He has worked on fusion neutronics for more than 20 years, and he planned and constructed the Fusion Neutronics Source (FNS) facility. He served as the Japanese leader of the JAERI/U.S. Department of Energy (U.S. DOE) collaboration on fusion blanket neutronics. His recent research has focused on International Fusion Materials Irradiation Facility conceptual design activities.

Tomoo Nakamura (BS, physics, Kyoto University, Japan, 1957) is currently director of the Public Acceptance Database Center, Research Organization for Information Science and Technology. His research background includes experimental reactor physics on fast breeder reactors and nuclear technology on fusion reactor blankets. He served as the former Japanese leader of the JAERI/U.S. DOE collaboration on fusion blanket neutronics.

Mohamed A. Abdou is a professor in the Department of Mechanical, Aerospace, and Nuclear Engineering at the University of California, Los Angeles (UCLA) and also is the director of fusion technology at UCLA. His research interests include neutronics, thermomechanics, fusion technology, and reactor design and analysis. He served as the U.S. leader of the JAERI/U.S. DOE collaboration on fusion blanket neutronics.

E. F. Bennett (PhD, University of New Hampshire, 1957) is a physicist at Argonne National Laboratory. He has been a section head of experimental reactor physics since 1970. He is best known as the inventor of a widely used in-core proton-recoil spectrometer—a technique that he has been continually updating. He has also made contributions to the field of reactivity measurement by reactor noise techniques, in particular, by providing a common theoretical basis and introducing a new type of variance experiment.

Anil Kumar (PhD, University of Bombay, India, 1981) is senior development engineer at UCLA. His current research interests include fusion reactor nucleonics experiments and analysis, technique development for nuclear heating, decay heat measurements, biological dose, fusion diagnostics, safety factor methodology for fusion reactor design parameters, low-activation materials, inertial confinement fusion, and sequential reactions. He has conducted experiments at leading facilities such as the FNS facility in Japan, the Tokamak Fusion Test Reactor (TFTR) at Princeton University, and LOTUS in Switzerland.

Yoichi Watanabe (PhD, nuclear engineering, University of Wisconsin-Madison) is currently a research fellow at Memorial Sloan-Kettering Cancer Center in New York City and specializes in radiation physics and radiotherapy physics. He has done research in fusion engineering, space nuclear power engineering, and nuclear plasma physics.

Mahmoud Z. Youssef (PhD, nuclear engineering, University of Wisconsin, 1980) is a senior research engineer in the Department of Mechanical, Aerospace, and Nuclear Engineering at UCLA. He participated in several conceptual magnetic fusion energy and inertial fusion energy reactor design studies with emphasis on nuclear analysis and blanket/shield design. His research interests are in the areas of blanket/shield design optimization, nuclear data, sensitivity/uncertainty studies, neutronics methods and code development, tritium fuel cycle, radioactivity and safety aspects of fusion, integral experiments, neutronics testing, and research and development for fusion reactors, particularly the International Thermonuclear Experimental Reactor (ITER).